

Measuring Trilinear Higgs Couplings in the MSSM^{*}

P. Osland^a and P. N. Pandita^b

^a Department of Physics, University of Bergen, N-5007 Bergen, Norway

^b Department of Physics, North Eastern Hill University, Shillong 793 022, India

Abstract

Trilinear couplings of the neutral CP -even Higgs bosons in the Minimal Supersymmetric Standard Model (MSSM) can be measured through the multiple production of the lightest CP -even Higgs boson (h) at high-energy e^+e^- colliders. This includes the production of the heavier CP -even Higgs boson (H) via $e^+e^- \rightarrow ZH$, in association with the CP -odd Higgs boson (A) in $e^+e^- \rightarrow AH$, or via $e^+e^- \rightarrow \nu_e \bar{\nu}_e H$, with H subsequently decaying through $H \rightarrow hh$. These processes can enable one to measure the trilinear Higgs couplings λ_{Hhh} and λ_{hhh} , which can be used to theoretically reconstruct the Higgs potential. We delineate the regions of the MSSM parameter space in which these trilinear Higgs couplings could be measured.

1 Introduction

Supersymmetry is at present the only known framework in which the Higgs sector [1] of the Standard Model (SM), so crucial for its internal consistency, is natural [2]. The minimal version of the Supersymmetric Standard Model (MSSM) contains two Higgs doublets (H_1, H_2) with opposite hypercharges: $Y(H_1) = -1$, $Y(H_2) = +1$, so as to generate masses for up- and down-type quarks (and leptons), and to cancel gauge anomalies. After spontaneous symmetry breaking induced by the neutral components of H_1 and H_2 obtaining vacuum expectation values, $\langle H_1 \rangle = v_1$, $\langle H_2 \rangle = v_2$, $\tan \beta = v_2/v_1$, the MSSM contains two neutral CP -even (h, H), one neutral CP -odd (A), and two charged (H^\pm) Higgs bosons [1]. Because of gauge invariance and supersymmetry, all the Higgs masses and the Higgs couplings in the MSSM can be described (at tree level) in terms of only two parameters, which are usually chosen to be $\tan \beta$ and m_A , the mass of the CP -odd Higgs boson.

In particular, all the trilinear self-couplings of the physical Higgs particles can be predicted theoretically (at the tree level) in terms of m_A and $\tan \beta$. Once a light Higgs boson is discovered, the measurement of these trilinear couplings can be used to reconstruct the Higgs potential of the MSSM. This will go a long way toward establishing the Higgs mechanism as the basic mechanism of spontaneous symmetry breaking in gauge theories. Although the measurement of all the Higgs couplings in the MSSM is a difficult task,

^{*}Presented at *VIIIth UNESCO St. Petersburg International School of Physics*, May 25 – June 4, 1998. To be published in the Proceedings

preliminary theoretical investigations by Plehn, Spira and Zerwas [3], and by Djouadi, Haber and Zerwas (DHZ) [4], of the measurement of these couplings at the LHC and at a high-energy e^+e^- linear collider, respectively, are encouraging.

We have considered in detail [5] the question of possible measurements of the trilinear Higgs couplings of the MSSM at a high-energy e^+e^- linear collider. We assume that such a facility will operate at an energy of 500 GeV with an integrated luminosity per year of $\mathcal{L}_{\text{int}} = 500 \text{ fb}^{-1}$ [6]. (This is a factor of 10 more than the earlier estimate.) In a later phase one may envisage an upgrade to an energy of 1.5 TeV.

The trilinear Higgs couplings that are of interest are λ_{Hhh} , λ_{hhh} , and λ_{hAA} , involving both the CP -even and CP -odd Higgs bosons. The couplings λ_{Hhh} and λ_{hhh} are rather small with respect to the corresponding trilinear coupling $\lambda_{hhh}^{\text{SM}}$ in the SM (for a given mass of the lightest Higgs boson m_h), unless m_h is close to the upper value (decoupling limit). The coupling λ_{hAA} remains small for all parameters.

Throughout, we include one-loop radiative corrections [7] to the Higgs sector in the effective potential approximation. In particular, we take into account the parameters A and μ , the soft supersymmetry breaking trilinear parameter and the bilinear Higgs(ino) parameter in the superpotential, respectively, and as a consequence the left–right mixing in the squark sector, in our calculations. We thus include all the relevant parameters of the MSSM in our study [5]. Related work has recently been presented by Dubinin and Semenov [8].

For a given value of m_h , the values of these couplings significantly depend on the soft supersymmetry-breaking trilinear parameter A , as well as on μ , and thus on the resulting mixing in the squark sector. Since the trilinear couplings tend to be small, and depend on several parameters, their effects are somewhat difficult to estimate.

The dominant source of multiple production of the Higgs (h) boson, is through Higgsstrahlung of H , and through production of H in association with the CP -odd Higgs boson. This source of multiple production can be used to extract the trilinear Higgs coupling λ_{Hhh} . The non-resonant fusion mechanism for multiple h production, $e^+e^- \rightarrow \nu_e \bar{\nu}_e hh$, involves two trilinear Higgs couplings, λ_{Hhh} and λ_{hhh} , and is useful for extracting λ_{hhh} .

2 The Higgs Sector of the MSSM

At the tree level, the Higgs sector of the MSSM is described by two parameters, which can be conveniently chosen as m_A and $\tan \beta$ [1]. There are, however, substantial radiative corrections to the CP -even neutral Higgs masses and couplings [7, 9]. They are, in general, positive, and they shift the mass of the lightest MSSM Higgs boson upwards.

The Higgs mass falls rapidly at small values of $\tan \beta$. Since the LEP experiments are obtaining lower bounds on the mass of the lightest Higgs boson, they are beginning to rule out significant parts of the small- $\tan \beta$ parameter space, depending on the model assumptions. ALEPH finds a lower limit of $m_h > 72.2 \text{ GeV}$, irrespective of $\tan \beta$, and a limit of $\sim 88 \text{ GeV}$ for $1 < \tan \beta \lesssim 2$ [10]. We take $\tan \beta = 2$ to be a representative value.

3 Trilinear Higgs couplings

In units of $gm_Z/(2\cos\theta_W) = (\sqrt{2}G_F)^{1/2}m_Z^2$, the relevant tree-level trilinear Higgs couplings are given by

$$\lambda_{Hhh}^0 = 2\sin 2\alpha \sin(\beta + \alpha) - \cos 2\alpha \cos(\beta + \alpha), \quad (3.1)$$

$$\lambda_{hhh}^0 = 3\cos 2\alpha \sin(\beta + \alpha), \quad (3.2)$$

$$\lambda_{hAA}^0 = \cos 2\beta \sin(\beta + \alpha), \quad (3.3)$$

with α the mixing angle in the CP -even Higgs sector, which can be calculated in terms of the parameters appearing in the CP -even Higgs mass matrix. The dominant one-loop radiative corrections are proportional to $(m_t/m_W)^4$ [11].

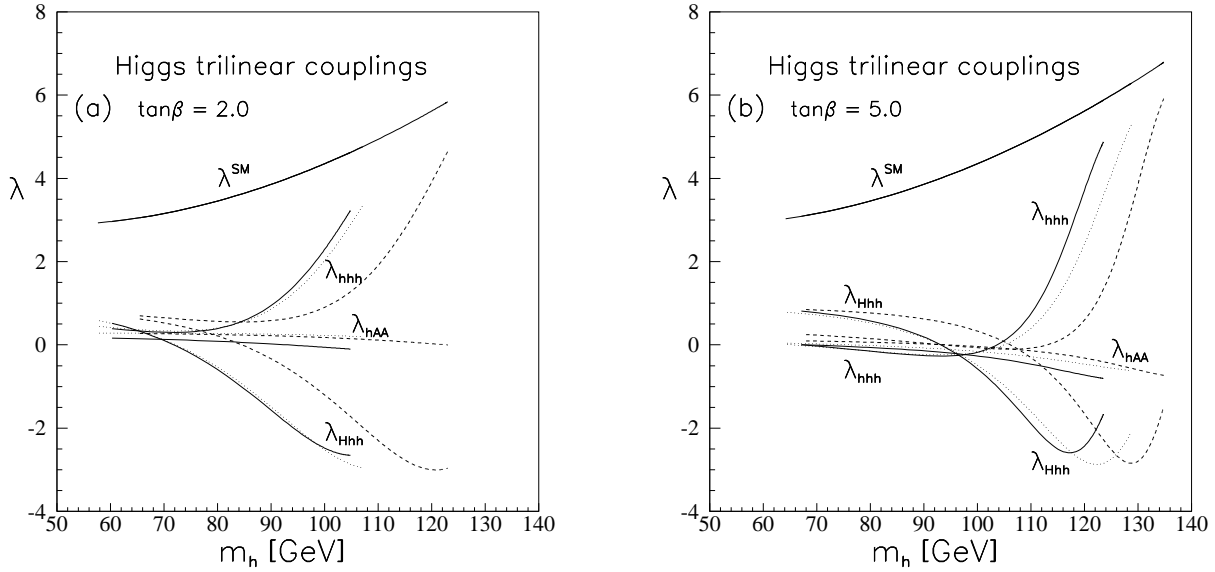


Figure 1: Trilinear Higgs couplings λ_{Hhh} , λ_{hhh} and λ_{hAA} as functions of m_h for two values of $\tan\beta$: (a) $\tan\beta = 2.0$, (b) $\tan\beta = 5.0$. Each coupling is shown for three cases of the mixing parameters: no mixing ($A = 0$, $\mu = 0$, solid), mixing with $A = 1$ TeV and $\mu = -1$ TeV (dotted), as well as $A = 1$ TeV and $\mu = 1$ TeV (dashed).

The trilinear couplings depend significantly on m_A , and thus also on m_h . This is shown in Fig. 1, where we compare λ_{Hhh} , λ_{hhh} and λ_{hAA} for three different values of $\tan\beta$, and the SM quartic coupling λ^{SM} (which also includes one-loop radiative corrections [12]).

At low values of m_h , the MSSM trilinear couplings are rather small. For some value of m_h the couplings λ_{Hhh} and λ_{hhh} start to increase in magnitude, whereas λ_{hAA} remains small. The values of m_h at which they start becoming significant depend crucially on $\tan\beta$. For $\tan\beta = 2$ (Fig. 1a) this transition takes place around $m_h \sim 90$ – 100 GeV, whereas for $\tan\beta = 5$ the critical value of m_h increases to 100 – 110 (see Fig. 1b). In this region, the actual values of λ_{Hhh} and λ_{hhh} (for a given value of m_h) change significantly if

A becomes large and positive. A non-vanishing squark-mixing parameter A is thus quite important. Also, for special values of the parameters, the couplings may vanish [13].

To sum up the behaviour of the trilinear couplings, we note that λ_{Hhh} and λ_{hhh} are small for $m_h \lesssim 100\text{--}120$ GeV, depending on the value of $\tan\beta$. However, as m_h approaches its maximum value, which is reached rapidly as m_A becomes large, $m_A \gtrsim 200$ GeV, these trilinear couplings become large. Thus, as functions of m_A , the trilinear couplings λ_{Hhh} and λ_{hhh} are large for most of the parameter space. We also note that, for large values of $\tan\beta$, λ_{Hhh} tends to be relatively small, whereas λ_{hhh} becomes large, if also m_A (or, equivalently, m_h) is large.

4 Production mechanisms

The different mechanisms for the multiple production of the MSSM Higgs bosons in e^+e^- collisions have been discussed by DHZ. The dominant mechanism for the production of multiple CP -even light Higgs bosons (h) is through the production of the heavy CP -even Higgs boson H , which then decays via $H \rightarrow hh$. The heavy Higgs boson H can be produced by H -strahlung, in association with A , and by the resonant WW fusion mechanism. These mechanisms for multiple production of h

$$\left. \begin{aligned} e^+e^- &\rightarrow ZH, AH \\ e^+e^- &\rightarrow \nu_e\bar{\nu}_e H \end{aligned} \right\}, \quad H \rightarrow hh, \quad (4.1)$$

are shown in Fig. 2. All the diagrams of Fig. 2 involve the trilinear coupling λ_{Hhh} .

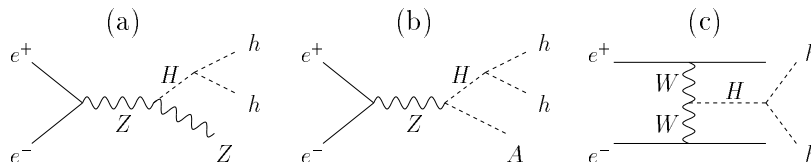


Figure 2: Feynman diagrams for the resonant production of hh final states in e^+e^- collisions.

A background to (4.1) comes from the production of the pseudoscalar A in association with h and its subsequent decay to hZ

$$e^+e^- \rightarrow hA, \quad A \rightarrow hZ, \quad (4.2)$$

leading to Zhh final states. A second mechanism for hh production is double Higgs-strahlung in the continuum with a Z boson in the final state,

$$e^+e^- \rightarrow Z^* \rightarrow Zhh. \quad (4.3)$$

We note that the non-resonant analogue of the Feynman diagram of Fig. 2b involves, apart from the coupling λ_{Hhh} , the trilinear Higgs coupling λ_{hhh} as well.

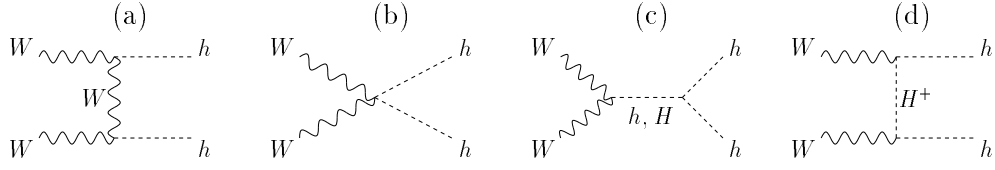


Figure 3: Feynman diagrams for the non-resonant WW fusion mechanism for the production of hh states in e^+e^- collisions.

Finally, there is a mechanism of multiple production of the lightest Higgs boson through non-resonant WW fusion in the continuum (see Section 7):

$$e^+e^- \rightarrow \bar{\nu}_e \nu_e W^* W^* \rightarrow \bar{\nu}_e \nu_e hh. \quad (4.4)$$

It is important to note that all the diagrams of Fig. 2 involve the trilinear coupling λ_{Hhh} only. On the other hand, the non-resonant analogue of Fig. 2b, and Fig. 3c involve both the trilinear Higgs couplings λ_{Hhh} and λ_{hhh} .

5 Higgs-strahlung and Associated Production of H

The dominant source for the production of multiple Higgs bosons (h) in e^+e^- collisions is through the production of the heavier CP -even Higgs boson H either via Higgs-strahlung or in association with A , followed, if kinematically allowed, by the cascade decay $H \rightarrow hh$. The cross sections for these processes can be found in [14, 15].

In Fig. 4 we plot the cross sections for the e^+e^- centre-of-mass energies $\sqrt{s} = 500$ GeV, as functions of the Higgs mass m_H and for $\tan\beta = 2.0$. For large values of the mass m_A of the pseudoscalar Higgs boson, all the Higgs bosons, except the lightest one (h), become heavy and decouple [16] from the rest of the spectrum.

At values of $\tan\beta$ that are not too large, the trilinear Hhh coupling λ_{Hhh} can be measured by the decay process $H \rightarrow hh$, which has a width proportional to λ_{Hhh}^2 . However, this is possible only if the decay is kinematically allowed, and the branching ratio is sizeable. In Fig. 5 we show the branching ratios (at $\tan\beta = 2$) for the main decay modes of the heavy CP -even Higgs boson as a function of the H mass. Apart from the hh decay mode, the other important decay modes are $H \rightarrow WW^*, ZZ^*$. We note that the couplings of H to gauge bosons can be measured through the production cross sections for $e^+e^- \rightarrow \nu_e \bar{\nu}_e H$; therefore the branching ratio $BR(H \rightarrow hh)$ can be used to measure the triple Higgs coupling λ_{Hhh} .

For increasing values of $\tan\beta$, the Hhh coupling gradually gets weaker (see Fig. 1), and hence the prospects for measuring λ_{Hhh} diminish. This is also indicated in Fig. 5, where we show the H branching ratios for $\tan\beta = 5$.

There is actually a sizeable region in the m_A - $\tan\beta$ plane where the decay $H \rightarrow hh$ is kinematically forbidden. This is shown in Fig. 6, where we also display the regions where

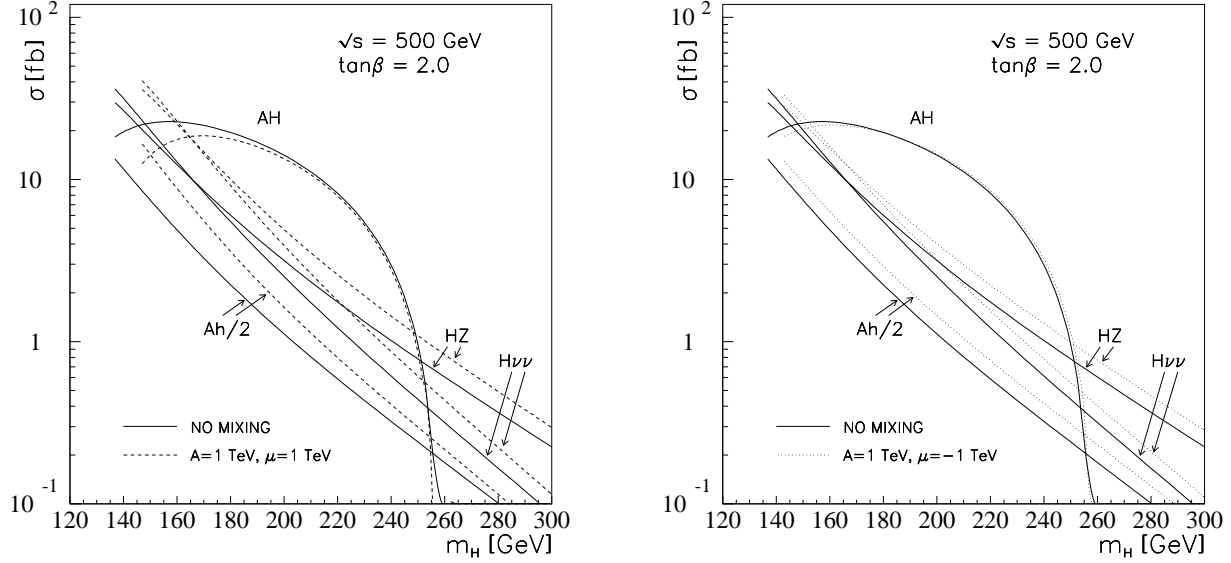


Figure 4: Cross sections for the production of the heavy Higgs boson H in e^+e^- collisions, and for the background process in which Ah is produced. Solid curves are for no mixing, $A = 0$, $\mu = 0$. Dashed and dotted curves refer to mixing, as indicated.

the $H \rightarrow hh$ branching ratio is in the range 0.1–0.9. Clearly, in the forbidden region, the λ_{Hhh} cannot be determined from resonant production.

6 Double Higgs-strahlung and Triple h Production

For small and moderate values of $\tan\beta$, the study of decays of the heavy CP -even Higgs boson H provides a means of determining the triple-Higgs coupling λ_{Hhh} . In order to extract the coupling λ_{hhh} , other processes involving two-Higgs (h) final states must be considered. The Zhh final states, which can be produced in the non-resonant double Higgs-strahlung $e^+e^- \rightarrow Zhh$, could provide one possible opportunity, since it involves the coupling λ_{hhh} . These non-resonant processes have also been investigated [4, 5].

We show in Fig. 7 the Zhh cross section, with $\tilde{m} = 1$ TeV. The structure around $m_h = 70$ GeV (in the case of no mixing) is due to the vanishing and near-vanishing of the trilinear coupling.

In the case of no mixing, there is a broad minimum from $m_h \simeq 78$ to 90 GeV, followed by an enhancement around $m_h \sim 90$ –100 GeV. This structure is due to the vanishing of the branching ratio for $H \rightarrow hh$, which is kinematically forbidden in the region $m_h \simeq 78$ –90 GeV, see Fig. 6 (this coincides with the opening up of the channel $H \rightarrow WW$), followed by an increase of the trilinear couplings. This particular structure depends considerably on the exact mass values m_H and m_h . Thus, it depends on details of the radiative corrections and on the mixing parameters A and μ .

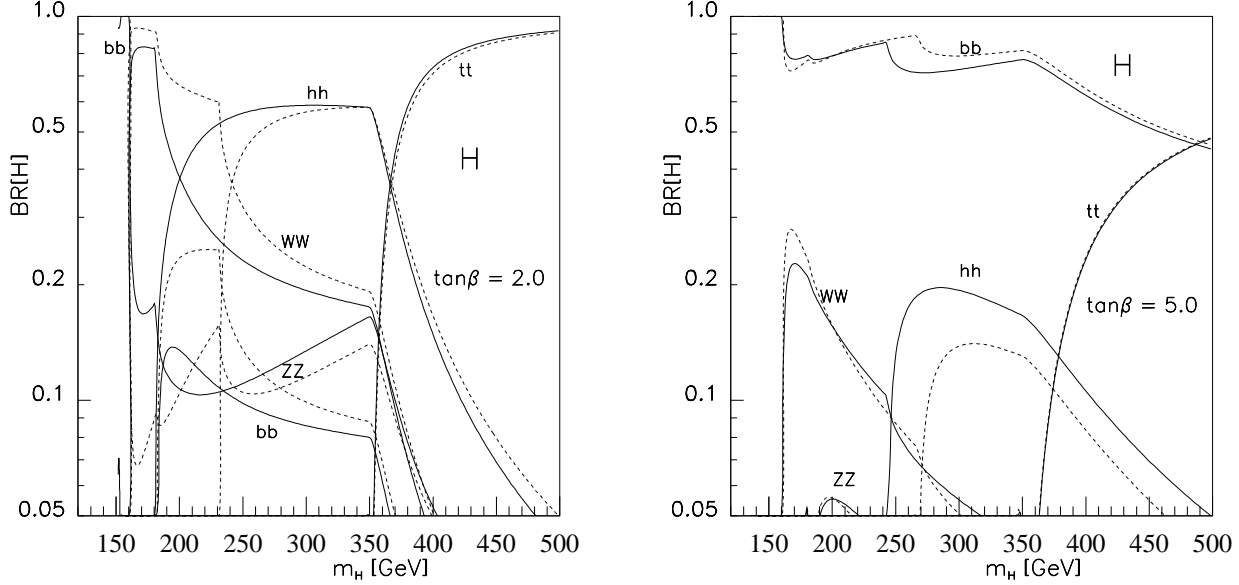


Figure 5: Branching ratios for the decay modes of the CP -even heavy Higgs boson H , for $\tan\beta = 2.0$ and 5.0 . Solid curves are for no mixing, $A = 0$, $\mu = 0$. Dashed and dotted curves refer to mixing, as indicated.

7 Fusion Mechanism for Multiple- h Production

A two-Higgs (hh) final state in e^+e^- collisions can also result from the WW fusion mechanism, which can either be a resonant process as in (4.1), or a non-resonant one like (4.4). Since the neutral-current couplings are smaller than the charged-current ones, the cross section for the ZZ fusion mechanism in (4.1) and (4.4) is an order of magnitude smaller than the WW fusion mechanism, and is here ignored.

The WW fusion cross section for $e^+e^- \rightarrow H\bar{\nu}_e\nu_e$ can be written as [17] (see also [5])

$$\sigma(e^+e^- \rightarrow H\bar{\nu}_e\nu_e) = \frac{G_F^3 m_W^4}{64\sqrt{2}\pi^3} \left[\int_{\mu_H}^1 dx \int_x^1 \frac{dy}{[1 + (y-x)/\mu_W]^2} \mathcal{F}(x, y) \right] \cos^2(\beta - \alpha). \quad (7.1)$$

This cross section is plotted in Fig. 4 for the centre-of-mass energy $\sqrt{s} = 500$ GeV, and for $\tan\beta = 2.0$, as a function of m_H . The resonant fusion mechanism, which leads to $[hh] + [\text{missing energy}]$ final states is competitive with the process $e^+e^- \rightarrow HZ \rightarrow [hh] + [\text{missing energy}]$, particularly at high energies. Since the dominant decay of h will be into $b\bar{b}$ pairs, the H -strahlung and the fusion mechanism will give rise to final states that will predominantly include four b -quarks. On the other hand, the process $e^+e^- \rightarrow AH$ will give rise to six b -quarks in the final state, since the AH final state typically yields three-Higgs $h[hh]$ final states.

Besides the resonant WW fusion mechanism for the multiple production of h bosons,

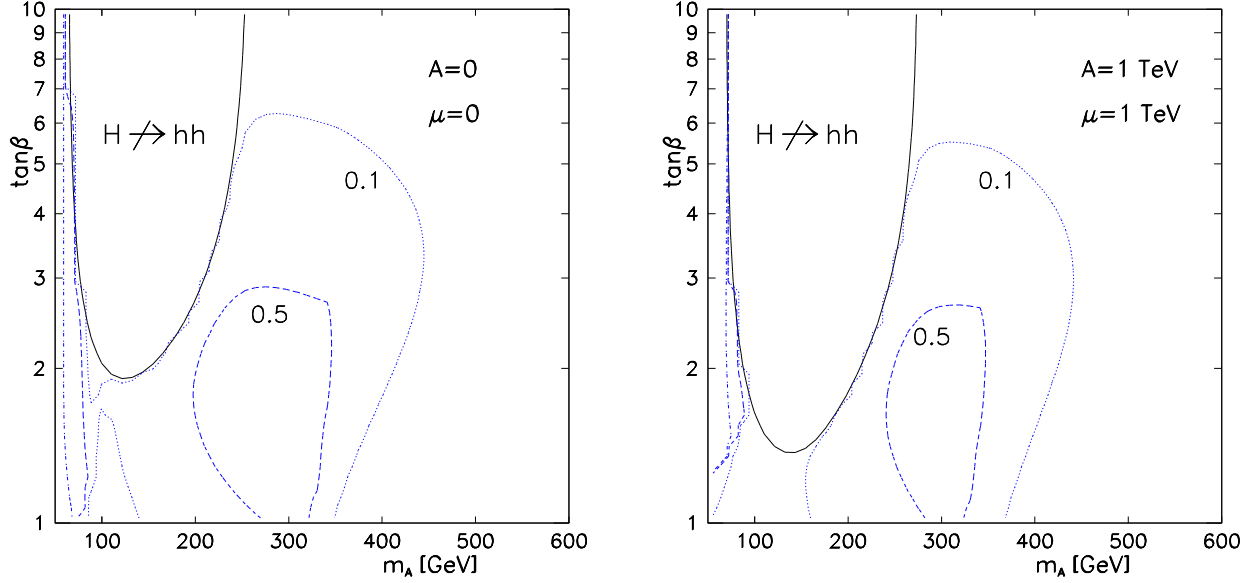


Figure 6: The region in the m_A - $\tan\beta$ plane where the decay $H \rightarrow hh$ is kinematically *forbidden* is indicated by a solid line contour. Also given are contours at which the branching ratio equals 0.1 (dotted), 0.5 (dashed) and 0.9 (dash-dotted, at the far left).

there is also a non-resonant WW fusion mechanism:

$$e^+e^- \rightarrow \nu_e \bar{\nu}_e hh, \quad (7.2)$$

through which the same final state of two h bosons can be produced. The cross section for this process, which arises through WW exchange as indicated in Fig. 3, can be written in the “effective WW approximation” as

$$\sigma(e^+e^- \rightarrow \nu_e \bar{\nu}_e hh) = \int_{\tau}^1 dx \frac{dL}{dx} \hat{\sigma}_{WW}(x), \quad (7.3)$$

where $\tau = 4m_h^2/s$. Here, the cross section is written as a WW cross section, at invariant energy squared $\hat{s} = xs$, folded with the WW “luminosity” [18]:

$$\frac{dL(x)}{dx} = \frac{G_F^2 m_W^4}{2} \left(\frac{v^2 + a^2}{4\pi^2} \right)^2 \frac{1}{x} \left\{ (1+x) \log \frac{1}{x} - 2(1-x) \right\}, \quad (7.4)$$

where $v^2 + a^2 = 2$.

The WW cross section receives contributions from several amplitudes, according to the diagrams (a)–(d) in Fig. 3. We have evaluated these contributions [5].

Our approach differs from that of DHZ in that we do not project out the longitudinal degrees of freedom of the intermediate W bosons. Instead, we follow the approach of Ref. [19], where transverse momenta are ignored everywhere except in the W propagators.

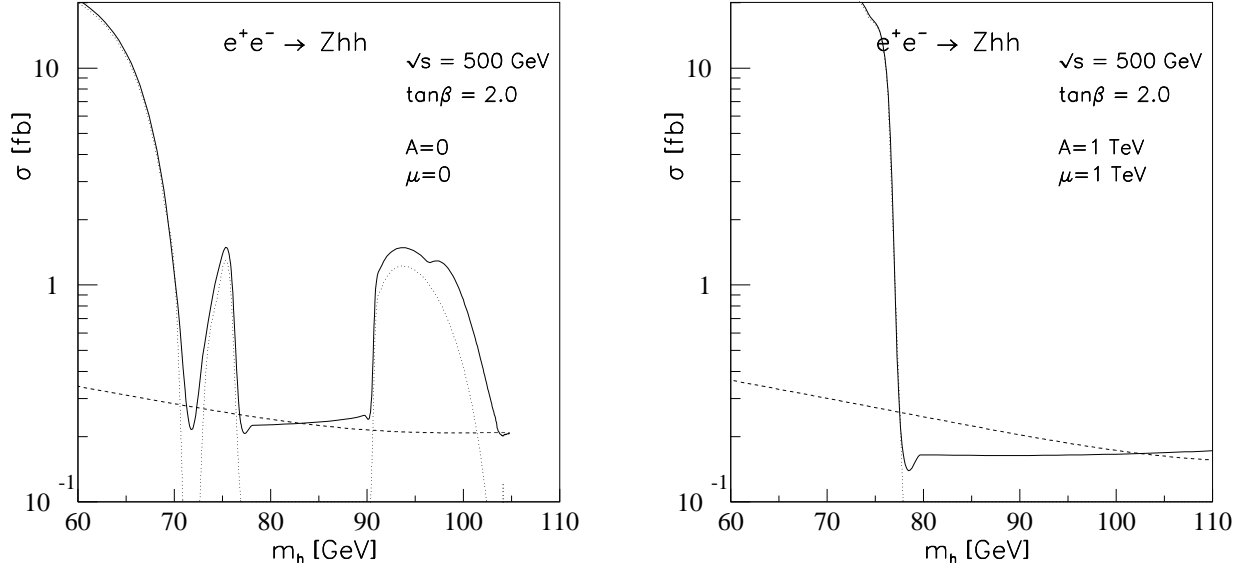


Figure 7: Cross section $\sigma(e^+e^- \rightarrow Zhh)$ as a function of m_h . The dotted curve is the resonant production, the dashed curve gives the decoupling limit.

We show in Fig. 8 the WW fusion cross section, at $\sqrt{s} = 1.5$ TeV, as given by Eqs. (7.1) and (7.3), with $\tilde{m} = 1$ TeV. The structure is reminiscent of Fig. 7, and the reasons for this are same. Notice, however, that the scale is different.

8 Sensitivity to λ_{Hhh} and λ_{hhh}

In Fig. 9 we have indicated in the m_A - $\tan \beta$ plane the regions where λ_{Hhh} and λ_{hhh} might be measurable for $\sqrt{s} = 500$ GeV. We identify regions according to the following criteria [4, 5]:

- (i) Regions where λ_{Hhh} might become measurable are identified as those where $\sigma(H) \times \text{BR}(H \rightarrow hh) > 0.1$ fb (solid), with the simultaneous requirement of $0.1 < \text{BR}(H \rightarrow hh) < 0.9$ [see Figs. 5–6]. In view of the recent, more optimistic, view on the luminosity that might become available, we also give the corresponding contours for 0.05 fb (dashed) and 0.01 fb (dotted).
- (ii) Regions where λ_{hhh} might become measurable are those where the *continuum* $WW \rightarrow hh$ cross section [Eq. (7.3)] is larger than 0.1 fb (solid). Also included are contours at 0.05 (dashed) and 0.01 fb (dotted).

Such regions are given for two cases of the mixing parameters A and μ , as indicated. We have excluded from the plots the region where $m_h < 72.2$ GeV, according to the LEP lower bound [10]. This corresponds to low values of m_A .

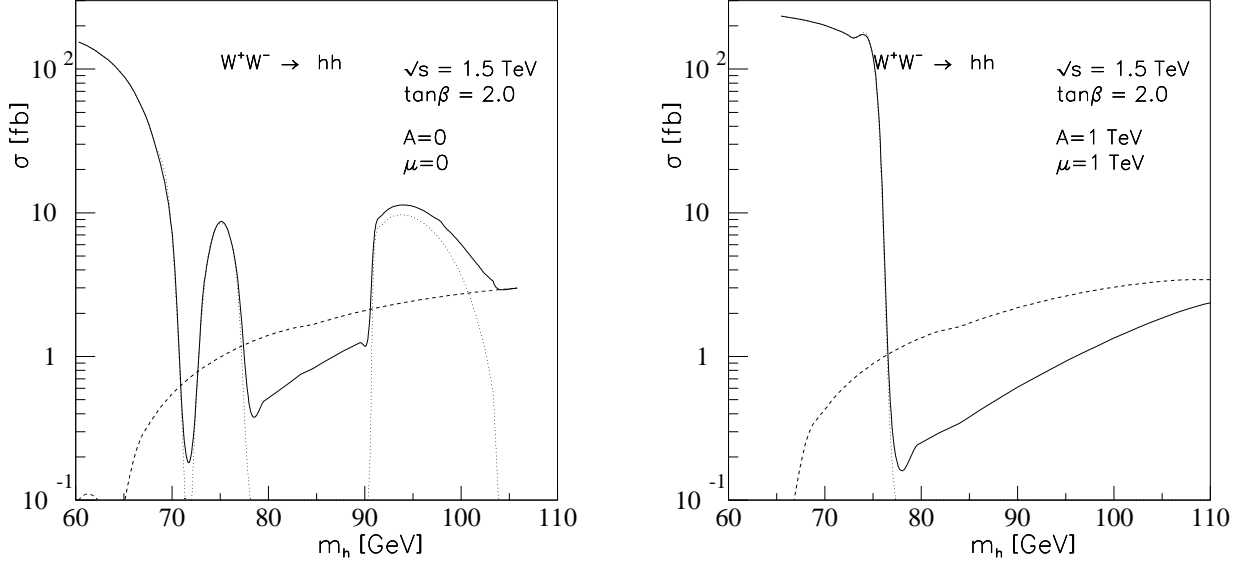


Figure 8: Cross section $\sigma(e^+e^- \rightarrow \nu_e \bar{\nu}_e hh)$ (via WW fusion) as a function of m_h . The dotted curve is the resonant production, the dashed curve gives the decoupling limit.

With an integrated luminosity of 500 fb^{-1} , the contours at 0.1 fb correspond to 50 events per year. This will of course be reduced by efficiencies, but should indicate the order of magnitude that can be reached.

At $\sqrt{s} = 500 \text{ GeV}$, with a luminosity of 500 fb^{-1} per year, the trilinear coupling λ_{Hhh} is accessible in a considerable part of the m_A - $\tan\beta$ parameter space: at m_A of the order of 200–300 GeV and $\tan\beta$ up to the order of 5. With increasing luminosity, the region extends somewhat to higher values of m_A . The “steep” edge around $m_A \simeq 200 \text{ GeV}$ (where increased luminosity does not help) is determined by the vanishing of $\text{BR}(H \rightarrow hh)$, see Fig. 6.

The coupling λ_{hhh} is accessible in a much larger part of this parameter space, but with a moderate luminosity, “large” values of $\tan\beta$ are accessible only if A is small.

It should be stressed that the requirements discussed here are necessary, but not sufficient conditions for the trilinear couplings to be measurable. We also note that there might be sizable corrections to the WW approximation, and that it would be desirable to incorporate the dominant two-loop corrections to the trilinear couplings.

9 Conclusions

We have presented the results of a detailed investigation [5] of the possibility of measuring the MSSM trilinear couplings λ_{Hhh} and λ_{hhh} at an e^+e^- collider. Where there is an overlap, we have confirmed the results of Ref. [4]. Our emphasis has been on taking into account all the parameters of the MSSM Higgs sector. We have studied the importance of mixing in the squark sector, as induced by the trilinear coupling A and the bilinear

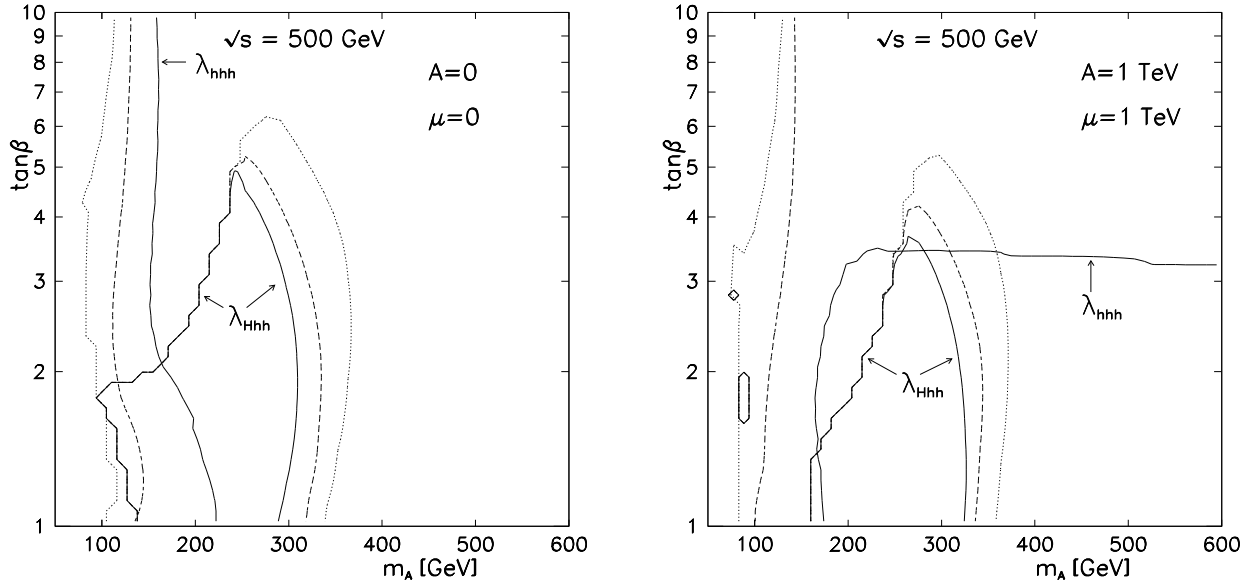


Figure 9: Regions where trilinear couplings λ_{Hhh} and λ_{hhh} might be measurable at $\sqrt{s} = 500$ GeV. Inside contours labelled λ_{Hhh} , $\sigma(H) \times \text{BR}(H \rightarrow hh) > 0.1$ fb (solid), while $0.1 < \text{BR}(H \rightarrow hh) < 0.9$. Inside (to the right or below) contour labelled λ_{hhh} , the *continuum* $WW \rightarrow hh$ cross section exceeds 0.1 fb (solid). Analogous contours are given for 0.05 (dashed) and 0.01 fb (dotted). Two cases of mixing are considered, as indicated.

coupling μ .

At moderate energies ($\sqrt{s} = 500$ GeV) the range in the m_A - $\tan\beta$ plane that is accessible for studying λ_{Hhh} changes quantitatively for non-zero values of the parameters A and μ . As far as the coupling λ_{hhh} is concerned, however, there is a qualitative change from the case of no mixing in the squark sector. If A is large, then high luminosity is required to reach “high” values of $\tan\beta$. At higher energies ($\sqrt{s} = 1.5$ TeV), the mixing parameters A and μ change the accessible region of the parameter space only in a quantitative manner.

This research was supported by the Research Council of Norway, and (PNP) by the University Grants Commission, India under project number 10-26/98(SR-I).

References

- [1] J. F. Gunion, H. E. Haber, G. Kane and S. Dawson, *The Higgs Hunter’s Guide*, Addison-Wesley, New York, 1990.
- [2] For reviews, see H.-P. Nilles, Phys. Rep. **110**, 1 (1984); H. E. Haber and G. L. Kane, Phys. Rep. **C117**, 75 (1985); R. Barbieri, Riv. Nuovo Cimento **11** No. 4, p. 1 (1988).
- [3] T. Plehn, M. Spira and P. M. Zerwas, Nucl. Phys. **B479**, 46 (1996).

- [4] A. Djouadi, H. E. Haber and P. M. Zerwas, Phys. Lett. **B375**, 203 (1996) and Erratum, to be published.
- [5] P. Osland and P. N. Pandita, CERN-TH/98-189, to appear in Phys. Rev. D, (Archive: hep-ph/9806351).
- [6] E. Accomando et al., Phys. Rep. **299**, 1 (1998). The luminosity quoted there is now believed to be too conservative.
- [7] J. Ellis, G. Ridolfi and F. Zwirner, Phys. Lett. **B257**, 83 (1991); Y. Okada, M. Yamaguchi and T. Yanagida, Prog. Theor. Phys. **85**, 1 (1991); H. E. Haber and R. Hempfling, Phys. Rev. Lett. **66**, 1815 (1991).
- [8] M. N. Dubinin and A. V. Semenov, hep-ph/9812246
- [9] J. Ellis, G. Ridolfi and F. Zwirner, Phys. Lett. **B262**, 477 (1991); R. Hempfling and A. H. Hoang, Phys. Lett. **B331**, 99 (1994); M. Carena, J.R. Espinosa, M. Quirós and C.E.M. Wagner, Phys. Lett. **B355**, 209 (1995); M. Carena, M. Quirós and C.E.M. Wagner, Nucl. Phys. **B461**, 407 (1996); S. Heinemeyer, W. Hollik and G. Weiglein, Phys. Rev. **D58**, 091701 (1998).
- [10] R. Barate *et al.* (ALEPH Collaboration), CERN-EP-98-145, Sep 1998.
- [11] V. Barger, M. S. Berger, A. L. Stange and R. J. N. Phillips, Phys. Rev. **D45**, 4128 (1992).
- [12] A. Sirlin and R. Zucchini, Nucl. Phys. **B266**, 389 (1986).
- [13] A. Djouadi, J. Kalinowski and P. M. Zerwas, Z. Phys. **C70**, 435 (1996).
- [14] G. Pócsik and G. Zsigmond, Z. Phys. **C10**, 367 (1981).
- [15] J. F. Gunion, L. Roszkowski, A. Turski, H. E. Haber, G. Gamberini, B. Kayser, S. F. Novaes, F. Olness and J. Wudka, Phys. Rev. **D38**, 3444 (1988).
- [16] H. E. Haber, in Proceedings of the Conference on *Perspectives for Electroweak Interactions in $e^+ e^-$ Collisions*, Ringberg (Tegernsee), Germany, 1995; ed. B. A. Kniehl (World Scientific, Singapore, 1995) p. 219.
- [17] A. Djouadi, D. Haidt, B. A. Kniehl, B. Mele and P. M. Zerwas, in Proceedings, Workshop on *$e^+ e^-$ Collisions at 500 GeV: The Physics Potential*, Munich-Annecy-Hamburg (DESY 92-123 A, Hamburg, 1992).
- [18] R. N. Cahn and S. Dawson, Phys. Lett. **B136**, 196 (1984); S. Dawson, Nucl. Phys. **B249**, 42 (1984); M. Chanowitz and M. K. Gaillard, Phys. Lett. **B142**, 85 (1984); I. Kuss and H. Spiesberger, Phys. Rev. **D53**, 6078 (1996).
- [19] G. Altarelli, B. Mele and F. Pitolli, Nucl. Phys. **B287**, 205 (1987).